Inorg. Chem. **2002**, *41*, 507–512

Syntheses, Structures, and Properties of Trinuclear Complexes $[M(bpca)_2\{M'(hfac)_2\}_2]$, Constructed with the Complexed Bridging Ligand $[M(bpca)_2]$ [M, M′ = Ni(II), Mn(II); Cu(II), Mn(II); Fe(II), Mn(II); Ni(II), Fe(II); and Fe(II), Fe(II); Hbpca = Bis(2-pyridylcarbonyl)amine, Hhfac = Hexafluoroacetylacetone]

Asako Kamiyama, Tomoko Noguchi, Takashi Kajiwara, and Tasuku Ito*

Department of Chemistry, Graduate School of Science, Tohoku University, Aoba, Aramaki, Aoba-ku, Sendai 980-8578, Japan

Received July 10, 2001

Five trinuclear complexes $[M(bpca)_2\{M'(hfac)_2\}_2]$ (where **MM′$_2$** = **NiMn$_2$**, **CuMn$_2$**, **FeMn$_2$**, **NiFe$_2$**, and **FeFe$_2$**; Hbpca = bis(2-pyridylcarbonyl)amine; and Hhfac = hexafluoroacetylacetone) were synthesized almost quantitatively by the reaction of $[M(bpca)_2]$ and $[M'(hfac)_2]$ in 1:2 molar ratio, and their structures and magnetic properties were investigated. Three complexes, with M′ = Mn, crystallize in the same space group, $Pna2_1$, whereas two complexes, with M′ = Fe, crystallize in $P4_1$, and complexes within each set are isostructural to one another. In all complexes, $[M(bpca)_2]$ acts as a bis-bidentate bridging ligand to form a linear trinuclear complex in which three metal ions are arranged in the manner M′–M–M′. The central metal ion is in a strong ligand field created by the N_6 donor set, and hence the Fe(II) in the $\{Fe(bpca)_2\}$ moiety is in a low-spin state. The terminal metal ions (M′) are surrounded by O_6 donor sets with a moderate ligand field, which leads to the high-spin configuration of Fe(II). Three metal ions in all complexes are almost collinear, and metal–metal distances are ca. 5.5 Å. The magnetic behavior of **NiMn$_2$** and **NiFe$_2$** shows a weak ferromagnetic interaction between the central Ni(II) ion and the terminal Mn(II) or Fe(II) ions. In these complexes, σ-spin orbitals of the central Ni(II) ion and those of terminal metal ions have different symmetry about a 2-fold rotation axis through the $Ni–N_{amide}–M'_{terminal}$ atoms, and this results in orthogonality between the neighboring σ-spin orbitals and thus ferromagnetic interactions.

Introduction

In recent years, the chemistry of supramolecules containing transition metal ions has attracted much attention.[1−10] They often show interesting properties induced by direct or indirect M−M interactions such as novel magnetic behavior,[1] multistep multielectron redox,[2] and new reactivities based on cooperative effect of multimetal centers.[3] Many such compounds have been prepared by using either well-designed organic ligands or transition metal complex ligands.[4−7]

* Corresponding author. E-mail: ito@agnus.chem.tohoku.ac.jp.

(1) (a) Brechin, E. K.; Yoo, J.; Nakano, M.; Huffman, J. C.; Hendrickson, D. N.; Christou, G. *Chem. Commun.* **1999**, 783. (b) Aubin, S. M. J.; Dilley, N. R.; Pardi, L.; Krzystek, J.; Wemple, M. W.; Brunel, L.-C.; Maple, M. B.; Christou, G.; Hendrickson, D. N. *J. Am. Chem. Soc.* **1998**, *120*, 4991. (c) Aubin, S. M. J.; Wemple, M. W.; Adams, D. M.; Tsai, H.-L.; Christou, G.; Hendrickson, D. N. *J. Am. Chem. Soc.* **1996**, *118*, 7746.

(2) (a) Ito, T.; Hamaguchi, T.; Nagino, H.; Yamaguchi, T.; Kido, H.; Zavarine, I. S.; Richmond, T.; Washington, J.; Kubiak, C. P. *J. Am. Chem. Soc.* **1999**, *121*, 4625. (b) Kido, H.; Nagino, H.; Ito, T. *Chem. Lett.* **1996**, 745.

(3) (a) Uozumi, S.; Furutachi, H.; Ohba, M.; Okawa, H.; Fenton, D. E.; Shindo, K.; Murata, S.; Kitko, D. J. *Inorg. Chem.* **1998**, *37*, 6281. (b) Yamami, M.; Furutachi, H.; Yokoyama, T.; Okawa, H. *Inorg. Chem.* **1998**, *37*, 6832.

(4) (a) Ohba, M.; Usuki, N.; Fukita, N.; Okawa, H. *Angew. Chem., Int. Ed.* **1999**, *38*, 1795. (b) Zhong, Z. J.; Seino, H.; Mizobe, Y.; Hidai, M.; Fujishima, A.; Ohkoshi, S.; Hashimoto, K. *J. Am. Chem. Soc.* **2000**, *122*, 2952. (c) Larionova, J.; Gross, M.; Pilkington, M.; Andres, H.; Stoeckli-Evans, H.; Güdel, H. U.; Decurtins, S. *Angew. Chem., Int. Ed.* **2000**, *39*, 1605.

(5) (a) Pellaux, R.; Schmalle, H. W.; Huber, R.; Fischer, P.; Hauss, T.; Ouladdiaf, B.; Decurtins, S. *Inorg. Chem.* **1997**, *36*, 2301. (b) Mathonière, C.; Nuttall, C. J.; Carling, S. G.; Day, P. *Inorg. Chem.* **1996**, *35*, 1201. (c) Tamaki, H.; Zhong, Z. J.; Matsumoto, N.; Kida, S.; Koikawa, M.; Achiwa, N.; Hashimoto, Y.; Okawa, H. *J. Am. Chem. Soc.* **1992**, *114*, 6974.

(6) (a) Glaser, T.; Beissel, T.; Bill, E.; Weyhermüller, T.; Schünemann, V.; Meyer-Klaucke, W.; Trautwein, A. X.; Wieghardt, K. *J. Am. Chem. Soc.* **1999**, *121*, 2193. (b) Glaser, T.; Kesting, F.; Beissel, T.; Bill, E.; Weyhermüller, T.; Meyer-Klaucke, W.; Wieghardt, K. *Inorg. Chem.* **1999**, *38*, 722. (c) Krebs, C.; Glaser, T.; Bill, E.; Weyhermüller, T.; Meyer-Klaucke, W.; Wieghardt, K. *Angew. Chem., Int. Ed. Engl.* **1999**, *38*, 359.

10.1021/ic010731f CCC: $22.00
Published on Web 01/11/2002

It is well-known that a complex ligand is very useful for the construction of polynuclear complexes. The mononuclear $[M(bpca)_2]$ has been known for various divalent and trivalent transition metal ions [M(II) = Mn(II),[11] Fe(II),[12] Cu(II),[13] Zn(II),[13] and Rh(II);[14] M(III) = Fe(III),[12] Rh(III);[14] Hbpca = bis(2-pyridylcarbonyl)amine]. We demonstrated for the first time that $[M(bpca)_2]$ acts as a complex ligand to give trinuclear complexes of the type M′(μ-bpca)M(μ-bpca)M′ [M = Mn(II) and Fe(II), M′ = Mn(II)][8] and the two-dimensional complex $[Fe_2\{Ni(bpca)_2\}_3](ClO_4)_4$.[10] The trinuclear complexes M′(μ-bpca)M(μ-bpca)M′ would be suitable for the study of magnetic pathway if creating various combinations of M and M′ having dσ and/or dπ spin is possible. This study is undertaken from this viewpoint. We describe syntheses, structures, and magnetic properties of new trinuclear complexes $[M(bpca)_2\{M'(hfac)_2\}_2]$, which are abbreviated as **MM′$_2$** (Hhfac = hexafluoroacetylacetone). In this paper, we will discuss two complexes with terminal Mn(II) ions, **NiMn$_2$** and **CuMn$_2$**, and two complexes with terminal Fe(II) ions, **NiFe$_2$** and **FeFe$_2$**. Detailed studies on $[Fe(bpca)_2\{Mn(hfac)_2\}_2]$ (**FeMn$_2$**), which was reported previously,[8] are also presented for comparison. A revised synthetic method of the free Hbpca ligand is also reported.

Experimental Section

Synthesis. All chemicals were reagent grade and used as received. $[Cu(bpca)_2]\cdot H_2O$[13] and $[Fe(hfac)_2(H_2O)_2]$[15] were prepared by the literature methods. $[Fe(bpca)_2]\cdot H_2O$, also prepared by the literature methods,[12] was recrystallized from $CHCl_3$, and anhydrous $[Fe(bpca)_2]$ was obtained as black crystals.[16]

Preparation of Hbpca. 1,3,5-Tris(2-pyridyl)triazine (1.25 g, 4.0 mmol) was allowed to react with 2.0 g of copper sulfate pentahydrate (8.0 mmol) in 30 mL of water. The suspension was refluxed for 30 min, and from the resulting solution, blue microcrystals of $[Cu(bpca)(H_2O)_2][Cu(bpca)(SO_4)(H_2O)]H_2O$[17] were obtained (yield 1.4 g, 70%). Free organic ligand was isolated from this copper(II) complex. The copper(II) complex (1.0 g, 1.3 mmol) and 2.0 g of Na_2H_2edta (5.4 mmol) were vigorously stirred for 1 h in a water (80 mL) and chloroform (50 mL) mixture at room temperature. The light green organic layer was dried over sodium sulfate and was evaporated to dryness to give slightly colored solids. Colorless prisms of 3Hbpca·1,4-dioxane were obtained by recrystallization of the residue from hot 1,4-dioxane solution. This compound was filtered and dried in vacuo to give white powder of Hbpca (yield ~80%). Anal. Calcd for $C_{12}H_9N_3O_2$: C, 63.43; H, 3.99; N, 18.49. Found: C, 63.40; H, 4.11; N, 18.25.

Preparation of [Ni(bpca)$_2$]. A solution of Hbpca (287 mg, 1.25 mmol) in acetone (40 mL) and $Ni(NO_3)_2\cdot 6H_2O$ (291 mg, 1 mmol) in water (20 mL) were mixed with stirring. Orange microcrystals[18] were obtained by slow evaporation at room temperature, collected by filtration, and dried. Anal. Calcd for $C_{24}H_{16}N_6O_4Ni$: C, 56.40; H, 3.16; N, 16.40. Found: C, 55.80; H, 3.34; N, 16.20. IR (KBr, cm^{-1}): ν(C=O) 1695.

Preparation of Complexes NiMn$_2$ and CuMn$_2$. To a solution of $[Ni(bpca)_2]$ (10 mg, 0.02 mmol) in $CHCl_3$ (2 mL) was added $[Mn(hfac)_2(H_2O)_2]$ (20 mg, 0.04 mmol) in $CHCl_3$ (3 mL). Orange crystals of **NiMn$_2$** were obtained by slow evaporation at room temperature, which were filtered and dried in the air. Yield: 24 mg (82%). Green crystals of **CuMn$_2$** were obtained, in a manner similar to **NiMn$_2$**, with $[Cu(bpca)_2]\cdot H_2O$ instead of $[Ni(bpca)_2]$. Yield: 85%.

For **NiMn$_2$**: Anal. Calcd for $C_{44}H_{20}N_6O_{12}Mn_2NiF_{24}$: C, 36.50; H, 1.39; N, 5.80. Found: C, 36.30; H, 1.43; N, 5.79. IR (KBr, cm^{-1}): ν(C=O) 1650.

For **CuMn$_2$**: Anal. Calcd for $C_{44}H_{20}N_6O_{12}Mn_2CuF_{24}$: C, 36.40; H, 1.39; N, 5.78. Found: C, 36.60; H, 1.69; N, 5.78. IR (KBr, cm^{-1}): ν(C=O) 1650.

Preparation of Complex FeMn$_2$. The synthesis of **FeMn$_2$** was previously reported.[8]

Preparation of Complexes NiFe$_2$ and FeFe$_2$. Complexes **NiFe$_2$** and **FeFe$_2$** were prepared in a manner similar to **NiMn$_2$** and **FeMn$_2$**, respectively, except that $[Fe(hfac)_2(H_2O)_2]$ was used in place of $[Mn(hfac)_2(H_2O)_2]$. They were obtained as purple and black crystals, respectively. Yield: 88% for **NiFe$_2$** and 92% for **FeFe$_2$**.

For **NiFe$_2$**: Anal. Calcd for $C_{44}H_{20}N_6O_{12}Fe_2NiF_{24}$: C, 36.42; H, 1.39; N, 5.79. Found: C, 36.50; H, 1.51; N, 5.67. IR (KBr, cm^{-1}): ν(C=O) 1656.

For **FeFe$_2$**: Anal. Calcd for $C_{44}H_{20}N_6O_{12}Fe_3F_{24}$: C, 36.49; H, 1.39; N, 5.80. Found: C, 36.70; H, 1.64; N, 5.86. IR (KBr, cm^{-1}): ν(C=O) 1657.

X-ray Crystallography. X-ray data for all complexes were collected at low temperature (−70 to −90 °C) with a Bruker AXS SMART-1000/CCD area detector using graphite-monochromated Mo Kα radiation. The intensity data were empirically corrected for absorption by using the program SADABS.[19] For **NiMn$_2$**, **CuMn$_2$**, and **FeMn$_2$**, the Laue symmetry was determined to be *mmm*, and from the systematic absences the space group was shown to be acentric $Pna2_1$. For **NiFe$_2$** and **FeFe$_2$**, the Laue symmetry was determined to be 4/*m*, and the space group was selected as

(7) (a) Birkelbach, F.; Flörke, U.; Haupt, H.-J.; Butzlaff, C.; Trautwein, A. X.; Wieghardt, K.; Chaudhuri, P. *Inorg. Chem.* **1998**, *37*, 2000. (b) Krebs, C.; Winter, M.; Weyhermüller, T.; Bill, E.; Wieghardt, K.; Chaudhuri, P. *J. Chem. Soc., Chem. Commun.* **1995**, 1913.

(8) Kajiwara, T.; Ito, T. *J. Chem. Soc., Dalton Trans.* **1998**, 3351.

(9) Kajiwara, T.; Ito, T. *Mol. Cryst. Liq. Cryst.* **1999**, *335*, 73.

(10) Kamiyama, A.; Noguchi, T.; Kajiwara, T.; Ito, T. *Angew. Chem., Int. Ed.* **2000**, *39*, 3130.

(11) Marcos, D.; Folgado, J.-V.; Beltrán-Porter, D.; do Prado-Gambardella, M. T.; Pulcinelli, S. H.; de Almeida-Santos, R. H. *Polyhedron* **1990**, *9*, 2699.

(12) Wocadlo, S.; Massa, W.; Folgado, J.-V. *Inorg. Chim. Acta* **1993**, *207*, 199.

(13) Marcos, D.; Martinez-Mañez, R.; Folgado, J.-V.; Beltrán-Porter, A.; Beltrán-Porter, D.; Fuertes, A. *Inorg. Chim. Acta* **1989**, *159*, 11.

(14) (a) Paul, P.; Tyagi, B.; Bilakhiya, A. K.; Bhadbhade, M. M.; Suresh, E. *J. Chem. Soc., Dalton Trans.* **1999**, 2009. (b) Paul, P.; Tyagi, B.; Bilakhiya, A. K.; Bhadbhade, M. M.; Suresh, E.; Ramachandraiah, G. *Inorg. Chem.* **1998**, *37*, 5733. (c) Paul, P.; Tyagi, B.; Bhadbhade, M. M.; Suresh, E. *J. Chem. Soc., Dalton Trans.* **1997**, 2273.

(15) Bailey, N. A.; Fenton, D. E.; Gonzalez, M. S. L. *Inorg. Chim. Acta* **1984**, *88*, 125.

(16) Crystal data: $C_{24}H_{16}FeN_6O_4$, M = 508.28, T = 200(2) K, tetragonal, space group $P42_1c$, a = 8.8178(8) Å, c = 14.016(2) Å, U = 1089.8(2) Å^3, Z = 2, final R values are R1 = 0.0361, wR2 = 0.0640 for reflections with $I > 2\sigma(I)$ and R1 = 0.0578, wR2 = 0.0690 for all data. Selected bond distances (Å): Fe−N_{py} = 1.966(2), Fe−N_{amide} = 1.951(2), C−O = 1.226(3).

(17) Crystal data: $C_{24}H_{24}Cu_2N_6O_{12}S$, M = 747.63, T = 293(2) K, monoclinic, space group $P2_1$, a = 10.2615(16) Å, b = 13.0627(19) Å, c = 10.2806(16) Å, β = 102.368(4)°, U = 1346.1(4) Å^3, Z = 2, final R values are R1 = 0.0379, wR2 = 0.0705 for reflections with $I > 2\sigma(I)$ and R1 = 0.0550, wR2 = 0.0757 for all data.

(18) Crystal data: $C_{24}H_{16}N_6O_4Ni$, M = 511.14, T = 200(2) K, tetragonal, space group $P42_1c$, a = 8.8216(4), c = 14.1346(10) Å, U = 1099.96(11) Å^3, Z = 2, final R values are R1 = 0.0259, wR2 = 0.0632 for reflections with $I > 2\sigma(I)$ and R1 = 0.0282, wR2 = 0.0641 for all data. Selected bond distances (Å): Ni−N_{py} = 2.1001(15), Ni−N_{amide} = 2.0246(17), C−O = 1.224(2).

(19) Sheldrick, G. M. *SADABS. Program for Empirical Absorption Correction of Area Detector Data*; University of Göttingen: Germany, 1996.

Table 1. Crystallographic Data for [Ni(bpca)$_2${Mn(hfac)$_2$}$_2$] (**NiMn$_2$**), [Cu(bpca)$_2${Mn(hfac)$_2$}$_2$] (**CuMn$_2$**), and [Fe(bpca)$_2${Mn(hfac)$_2$}$_2$] (**FeMn$_2$**), [Ni(bpca)$_2${Fe(hfac)$_2$}$_2$] (**NiFe$_2$**), and [Fe(bpca)$_2${Fe(hfac)$_2$}$_2$] (**FeFe$_2$**)

	NiMn$_2$	**CuMn$_2$**	**FeMn$_2$**	**NiFe$_2$**	**FeFe$_2$**
formula	$NiMn_2C_{44}H_{20}F_{24}N_6O_{12}$	$CuMn_2C_{44}H_{20}F_{24}N_6O_{12}$	$FeMn_2C_{44}H_{20}F_{24}N_6O_{12}$	$NiFe_2C_{44}H_{20}F_{24}N_6O_{12}$	$Fe_3C_{44}H_{20}F_{24}N_6O_{12}$
Fw	1449.25	1539.58	1446.39	1451.07	1448.21
crystal system	orthorhombic	orthorhombic	orthorhombic	tetragonal	tetragonal
space group	$Pna2_1$	$Pna2_1$	$Pna2_1$	$P4_1$	$P4_1$
a, Å	16.8287(11)	16.9340(9)	16.6214(10)	16.5975(8)	16.5136(7)
b, Å	20.1393(14)	20.1064(9)	20.0138(13)		
c, Å	16.2498(11)	16.2375(8)	16.2297(10)	18.8733(12)	18.5718(11)
V, Å^3	5507.4(6)	5528.6(5)	5398.9(6)	5199.2(5)	5064.5(4)
Z	4	4	4	4	4
T, °C	−80	−70	−73	−70	−90
radiation (λ, Å)	Mo Kα (0.7107 3)	Mo Kα (0.7107 3)	Mo Kα (0.7107 3)	Mo Kα (0.7107 3)	Mo Kα (0.7107 3)
ρ_{calc}, Mg/m^3	1.748	1.850	1.779	1.854	1.899
μ, mm^{-1}	0.935	0.992	0.874	1.063	1.006
R1[a], wR2[b] ($I > 2\sigma(I)$)	0.0505, 0.1173	0.0382, 0.0736	0.0465, 0.1122	0.0635, 0.1496	0.0415, 0.1020
R1[a], wR2[b] (all data)	0.0805, 0.1285	0.0813, 0.0838	0.0719, 0.1230	0.1100, 0.1765	0.0609, 0.1119

[a] $R1 = \sum||F_o| - |F_c||/\sum|F_o|$. [b] $wR2 = [\sum w(F_o^2 - F_c^2)^2/\sum w(F_o^2)^2]^{1/2}$.

Scheme 1

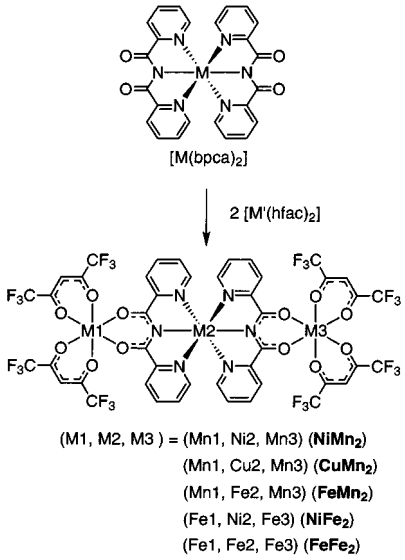

$P4_1$ from the two possibilities of $P4_1$ and $P4_3$. The structures were solved by the Patterson method using DIRDIF94 (PATTY),[20] and the structure refinement was carried out using full-matrix least-squares (SHELXL-93[21]) with absolute structure parameters of −0.008(14), 0.019(10), −0.021(16), 0.54(3), and 0.62(2) for complexes **NiMn$_2$**, **CuMn$_2$**, **FeMn$_2$**, **NiFe$_2$**, and **FeFe$_2$**, respectively. Non-hydrogen atoms were refined anisotropically, while the hydrogen atoms were treated using the riding model. Final crystallographic data and values of R1 and wR2 are listed in Table 1.

Measurements. Fourier transform infrared spectroscopy on KBr pellets was performed on a JASCO FT/IR-620 instrument.

Variable-temperature magnetic susceptibility measurements were made by using a SQUID magnetometer MPMS 5S (Quantum Design) at 1 T field for **NiMn$_2$**, **FeMn$_2$**, and **FeFe$_2$** and 0.5 T field for **NiFe$_2$**. Diamagnetic correction for each sample was determined from Pascal's constants.

(20) Beurskens, P. T.; Admiraal, G.; Bosman, W. P.; Gelder, R. D.; Israel, R.; Smits, J. M. M. *The DIRDIF-94 program system*; Technical Report of the Crystallography Laboratory: University of Nijmegen, The Netherlands, 1994.
(21) Sheldrick, G. M. *SHELXL93. Program for the Refinement of Crystal Structures*; University of Göttingen: Germany, 1993.

Results and Discussion

Syntheses. We already demonstrated that the four carbonyl groups of complex ligand [M(bpca)$_2$] can coordinate to metal ions to give polynuclear complexes.[8−10] Trinuclear complexes [M(bpca)$_2${M′(hfac)$_2$}$_2$] were obtained by the reaction of [M(bpca)$_2$] and [M′(hfac)$_2$]. There are two reasons for use of [M′(hfac)$_2$] as an acceptor. First, [M′(hfac)$_2$] is a good acceptor, due to the electron-withdrawing nature of the hfac$^-$ ligand. Second, the polymerization can be prevented because [M′(hfac)$_2$] has only two coordination-free sites. In fact, good crystalline compounds were obtained almost quantitatively in some M−M′ combinations.

From the combination of [M(bpca)$_2$] [M = Ni(II), Cu(II), Mn(II), Fe(II)] and [M′(hfac)$_2$] [M′ = Mn(II), Fe(II)], eight different trinuclear complexes were expected, but only six compounds (**NiMn$_2$**, **CuMn$_2$**, **MnMn$_2$**,[8] **FeMn$_2$**,[8] **NiFe$_2$**, and **FeFe$_2$**) were obtained, while **CuFe$_2$** and **MnFe$_2$** did not form. The reaction of [Cu(bpca)$_2$] and [Fe(hfac)$_2$] did not afford the desired **CuFe$_2$** complex but resulted in the precipitation of black crystals, which were determined to be **FeFe$_2$** by X-ray crystallography. In this reaction, a ligand substitution likely occurred between [Cu(bpca)$_2$] and [Fe(hfac)$_2$], and the resulting [Fe(bpca)$_2$] reacted with the remaining [Fe(hfac)$_2$] to give the trinuclear **FeFe$_2$** complex. The reaction of [Mn(bpca)$_2$] and [Fe(hfac)$_2$] was intractable. Possibly a similar ligand substitution reaction takes place. **CuFe$_2$** and **MnFe$_2$** did not form due to the low coordination affinity of the N_3 donor set in bpca$^-$ ligand to Cu(II) and Mn(II) ions. Aromatic nitrogen donor atoms show markedly stronger affinity to Fe(II) ion than Cu(II) and Mn(II) ions, and hence, [Fe(hfac)$_2$] undergoes a ligand exchange reaction to generate inert [Fe(bpca)$_2$] with short and stable Fe−N_{py} and Fe−N_{amide} bonds (vide infra).

Structures. The structure of **MnMn$_2$** was reported previously.[8] **MnMn$_2$**, **NiMn$_2$**, **CuMn$_2$**, and **FeMn$_2$** crystallize in the same space group, $Pna2_1$, and both **NiFe$_2$** and **FeFe$_2$** crystallize in $P4_1$. Complexes within each set are isostructural to one another. Figures 1 and 2 show the structures of trinuclear complexes **NiMn$_2$** and **NiFe$_2$**, respectively. The crystallographic data are summarized in Table 1, the selected

Table 2. Selected Bond Distances (Å) for Six Trinuclear Complexes

	$NiMn_2$	**$CuMn_2$**	**$MnMn_2$**[a]	**$FeMn_2$**	**$NiFe_2$**	**$FeFe_2$**
M1, M3	Mn(II)	Mn(II)	Mn(II)	Mn(II)	Fe(II)	Fe(II)
M2	Ni(II)	Cu(II)	Mn(II)	Fe(II)	Ni(II)	Fe(II)
M1−M2	5.4786(9)	5.4972(7)	5.6811(8)	5.3946(11)	5.447(2)	5.3515(18)
M2−M3	5.5049(10)	5.5732(7)	5.6909(7)	5.4159(11)	5.440(2)	5.3391(18)
M2−N1	2.092(3)	2.106(3)	2.236(3)	1.965(4)	2.080(7)	1.979(4)
M2−N2	2.024(3)	2.009(3)	2.204(3)	1.944(4)	2.005(9)	1.933(6)
M2−N3	2.091(3)	2.102(3)	2.226(3)	1.974(4)	2.092(6)	1.983(4)
M2−N4	2.117(4)	2.276(3)	2.262(3)	2.000(5)	2.117(7)	1.965(4)
M2−N5	2.021(3)	2.051(3)	2.196(3)	1.948(4)	2.020(9)	1.925(7)
M2−N6	2.101(4)	2.265(3)	2.246(3)	1.952(5)	2.122(7)	1.961(4)
M1−O1	2.164(3)	2.163(2)	2.147(3)	2.171(4)	2.145(6)	2.139(4)
M1−O2	2.184(4)	2.182(3)	2.179(3)	2.189(4)	2.128(7)	2.129(4)
M1−O5	2.149(4)	2.145(3)	2.150(3)	2.128(5)	2.070(6)	2.070(4)
M1−O6	2.173(3)	2.178(3)	2.180(3)	2.184(4)	2.055(6)	2.064(4)
M1−O7	2.173(4)	2.148(3)	2.136(6)	2.175(5)	2.052(6)	2.059(4)
M1−O8	2.118(4)	2.119(3)	2.125(3)	2.139(5)	2.082(6)	2.083(4)
M3−O3	2.201(3)	2.188(2)	2.187(2)	2.209(4)	2.115(6)	2.124(4)
M3−O4	2.183(3)	2.161(3)	2.172(3)	2.181(4)	2.121(6)	2.131(4)
M3−O9	2.162(3)	2.165(3)	2.156(3)	2.177(4)	2.065(6)	2.070(4)
M3−O10	2.139(4)	2.134(3)	2.140(3)	2.164(4)	2.065(7)	2.057(4)
M3−O11	2.137(3)	2.128(2)	2.132(2)	2.111(4)	2.063(7)	2.063(4)
M3−O12	2.137(3)	2.131(3)	2.134(3)	2.115(4)	2.084(5)	2.078(3)
O1−C6	1.257(5)	1.217(4)	1.232(4)	1.248(6)	1.242(11)	1.234(7)
O2−C7	1.240(6)	1.238(4)	1.227(4)	1.240(6)	1.245(11)	1.245(8)
O3−C18	1.252(5)	1.233(4)	1.241(4)	1.258(6)	1.243(11)	1.236(7)
O4−C19	1.253(5)	1.238(4)	1.238(4)	1.246(6)	1.234(11)	1.236(7)

[a] Reference 8.

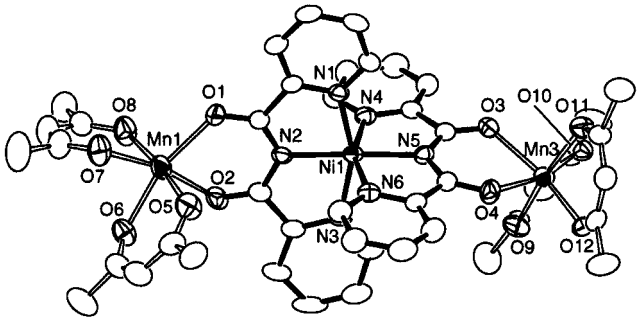

Figure 1. ORTEP drawings of **$NiMn_2$** with thermal ellipsoids at 50% probability. Hydrogen atoms and fluorine atoms are omitted for clarity. The moiety with solid bonds represents the {Ni(bpca)$_2$} unit.

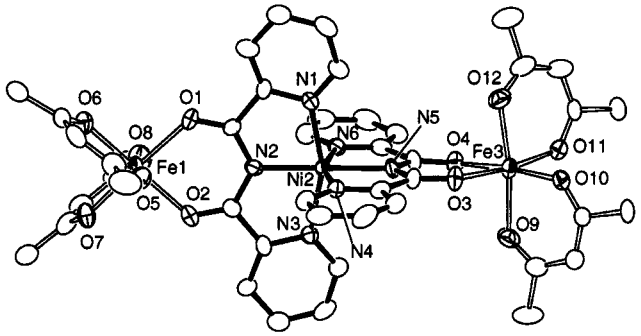

Figure 2. ORTEP drawings of **$NiFe_2$** with thermal ellipsoids at 50% probability. Hydrogen atoms and fluorine atoms are omitted for clarity. The moiety with solid bonds represents the {Ni(bpca)$_2$} unit.

bond distances for six trinuclear complexes are summarized in Table 2, and the selected bond angles are in Table S1 of the Supporting Information.

In all complexes, an {M(bpca)$_2$} unit binds two {M′(hfac)$_2$} units as a bridging bis-bidentate complex ligand to give a linear trinuclear complex (Scheme 1). When the six-membered chelate ring was formed, a slight structural change occurs on the O−C−N−C−O π system; C−O bonds in each trinuclear complex[22] elongate by about 0.02 Å as compared with that in the complex ligand [C−O = 1.224(2), 1.204(4)−1.217(5), and 1.226(3) Å for [Ni(bpca)$_2$],[18] [Cu(bpca)$_2$]·H_2O,[13] and [Fe(bpca)$_2$],[16] respectively]. In the parent mononuclear complex, the negative charge on the bpca$^-$ ligand is located essentially on the amide nitrogen N_{amide}, and carbonyl groups have double bond character. When the complex ligand coordinates to terminal metal ions, this minus charge delocalizes on the O−C−N−C−O conjugated system. Therefore, the double bond character diminishes, which leads to elongation of the C−O bonds. Such structural change was also detected by IR spectroscopy: the ν(C═O) stretching band shifts toward lower frequencies by ca. 40 cm^{-1} upon forming a trinuclear complex.

In all complexes, the central metal ion (M = Ni2 in **$NiMn_2$** and **$NiFe_2$**, Cu2 in **$CuMn_2$**, Mn2 in **$MnMn_2$**, Fe2 in **$FeMn_2$** and **$FeFe_2$**) is surrounded by four pyridyl nitrogens (N1, N3, N4, and N6) and two amide nitrogens (N2 and N5). The Fe−N distances in **$FeMn_2$** and **$FeFe_2$** are typical of low-spin Fe(II) complexes such as [Fe(bpca)$_2$]. Ni(II) and Fe(II) ions in four complexes were tightly bound in tetragonally distorted octahedral environment with axial Ni−N_{amide} = 2.005(9)−2.021(3) Å and Fe−N_{amide} = 1.925(7)−1.948(4) Å and equatorial Ni−N_{py} = 2.080(7)−2.122(7) Å and Fe−N_{py} = 1.965(7)−2.000(5) Å, respectively. On the other hand, Cu(II) and Mn(II) ions are loosely bound with the longest M−N distances of 2.265(3) Å and 2.246(3) Å, respectively. These trends were also found in parent mononuclear complexes. The bond distances around the metal ion in [M(bpca)$_2$] are summarized in Table 3. The long Cu−N distance is due to the Jahn−Teller distortion, whereas the

(22) The C−O distances in [Mn(bpca)$_2$] were not reported in ref 11.

Table 3. Bond Distances (Å) around Metal Ion in the Mononuclear Complexes [M(bpca)$_2$]

M	M−N$_{amide}$	M−N$_{py}$	M	M−N$_{amide}$	M−N$_{py}$
Ni(II)[a]	2.0246(17)	2.1001(15)	Mn(II)[c]	2.179(7)	2.216(7)
Cu(II)[b]	1.960(3)	2.084(3)		2.169(7)	2.255(7)
	1.997(3)	2.097(3)			2.285(8)
		2.305(3)			2.236(8)
		2.292(3)	Fe(II)[d]	1.951(2)	1.966(2)

[a] Reference 18. [b] Reference 13. [c] Reference 11. [d] Reference 16.

long Mn−N distance is of general feature for Mn(II) complexes with N-donor ligands. These facts show that the bpca$^-$ ligand has a stronger affinity for Ni(II) and Fe(II) ions than for Cu(II) and Mn(II) ions. As was mentioned already, the reaction of [Fe(hfac)$_2$] with [Mn(bpca)$_2$] or [Cu(bpca)$_2$] resulted in the ligand exchange to form [Fe(bpca)$_2$], and this fact also suggests the stronger affinity of bpca$^-$ for Fe(II) ion than for Cu(II) and Mn(II) ions. Upon forming the trinuclear complexes, slight elongation of M−N$_{amide}$ bonds is observed in **CuMn$_2$** and **MnMn$_2$**, which is caused by the decrease in the minus charge on the amide nitrogen (vide supra). In contrast, the same change of electronic distribution dose not affect on the tight binding Ni−N$_{amide}$ and reversely causes shortening of Fe−N$_{amide}$ distances (see Tables 2 and 3). In the latter case, π-back-donation from central low-spin Fe(II) ion to N$_{amide}$ increases with the decrease in the minus charge on N$_{amide}$.

Terminal Mn(II) ions in **NiMn$_2$**, **CuMn$_2$**, and **FeMn$_2$** and Fe(II) ions in **NiFe$_2$** and **FeFe$_2$** are surrounded by six oxygen atoms from two hfac$^-$ anions and from a {M(bpca)$_2$} unit. These two terminal metal ions in each trinuclear complex are in a chiral environment with the meso combination (Δ, Λ), and hence, the overall complexes are achiral. Mn−O bonds are rather long and are in the range of 2.116(4)−2.194(3) Å. Coordination polyhedra around the terminal Mn(II) ions are fairly distorted from ideal octahedron, possibly due to the spherical electronic configuration of Mn(II) ions ($^6A_1$) and loose Mn−O bonds. On the other hand, the Fe$_{terminal}$−O distances in **NiFe$_2$** and **FeFe$_2$** are typical of high-spin d^6 Fe(II) ions, showing that oxygen atoms are tightly bound to Fe(II) ions. The O$_6$ donor set in each terminal Fe(II) unit is close to a regular octahedron. These situations reflect on the M1−M2−M3 arrangement in the trinuclear complexes. The arrangement of three metal ions in each of **NiFe$_2$** and **FeFe$_2$** is almost linear [179.666(17)° and 179.737(17)°, respectively], whereas those in **NiMn$_2$**, **CuMn$_2$**, and **FeMn$_2$** are somewhat bent [169.099(16)°, 169.838(13)°, and 169.807(16)°, respectively].

Magnetic Properties. The temperature-dependent magnetic susceptibilities of five trinuclear complexes were measured down to 2 K. Here we report the magnetic behavior of two sets of trinuclear complexes (**NiMn$_2$**, **NiFe$_2$**, and **FeMn$_2$**, **FeFe$_2$**). **CuMn$_2$** did not show any significant magnetic interaction. Figure 3a displays $\chi_m T$ vs temperature data for the four compounds. The $\chi_m T$ values for **FeMn$_2$** vary slightly from 8.61 cm^3 K mol^{-1} at 300 K to 8.51 cm^3 K mol^{-1} at 20 K. **FeFe$_2$** shows a similar temperature dependence, with the $\chi_m T$ values in the range from 6.57 cm^3 K mol^{-1} at 300 K to 6.44 cm^3 K mol^{-1} at 50 K. In these

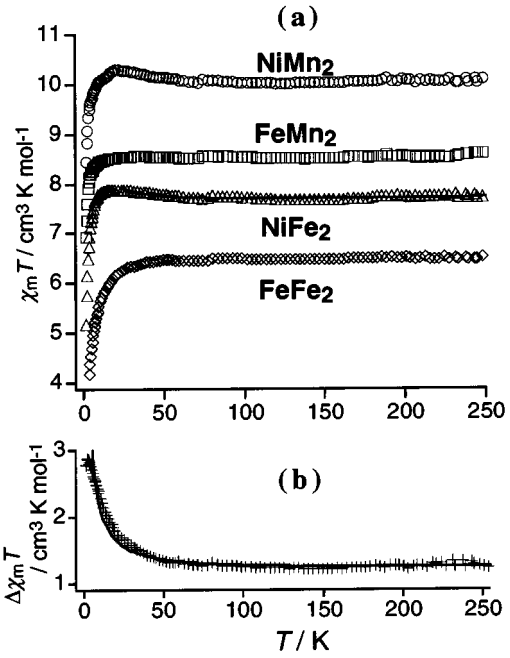

Figure 3. (a) Plots of $\chi_m T$ vs T for **NiMn$_2$** (○), **FeMn$_2$** (□), **NiFe$_2$** (△), and **FeFe$_2$** (◇). The solid line corresponds to the theoretical curve for which parameters are given in the text. (b) A plot of the difference in $\chi_m T$ ($\Delta\chi_m T = \chi_m T$ (**NiFe$_2$**) − $\chi_m T$ (**FeFe$_2$**)) as a function of temperature. The solid line is the theoretical curve with best-fit parameter given above.

complexes, the central Fe2 is in a divalent low-spin state, and the terminal Mn(II) ions in **FeMn$_2$** or the terminal Fe(II) ions in **FeFe$_2$** are magnetically independent. The data are consistent with 8.57 cm^3 K mol^{-1} and 6.49 cm^3 K mol^{-1} expected for two noncoupled spins of $S_{Mn1} = S_{Mn3} = 5/2$ with average $g = 1.98$ for **FeMn$_2$** and $S_{Fe1} = S_{Fe3} = 2$ with $g = 2.08$ for **FeFe$_2$**, respectively. Below 50 K, $\chi_m T$ for **FeFe$_2$** begins to fall, presumably due to the sizable zero-field splitting of the high-spin Fe(II) ions. Because of smaller zero-field splitting of Mn(II) ions, the reduction of $\chi_m T$ for **FeMn$_2$** begins at lower temperature.

The $\chi_m T$ values for **NiMn$_2$** show a slight increase on lowering the temperature from 10.08 cm^3 K mol^{-1} at 250 K, reaching the maximum value of 10.28 cm^3 K mol^{-1} at 24 K, and then continuously decrease.

For **NiFe$_2$**, the $\chi_m T$ value at 250 K, 7.71 cm^3 K mol^{-1}, is slightly larger than the spin-only value of 7.57 cm^3 K mol^{-1} for the dilute three magnetic centers with an average g value of 2.08. On lowering the temperature, the $\chi_m T$ values are retained, gradually increase below 63 K, reach 7.87 cm^3 K mol^{-1} at 19 K, and then decrease rapidly. The swift decrease of $\chi_m T$ values at low temperature is mainly due to the zero-field splitting of Ni(II) ion as well as two terminal Fe(II) ions.

These magnetic behaviors for **NiMn$_2$** and **NiFe$_2$** suggest ferromagnetic interactions between adjoining Ni(II) ion and Mn(II) ions or Fe(II) ions through the chelating O−C−N−C−O moiety. Magnetic data of these complexes were analyzed by the three-spin model with exchange coupling constant J [$H = -2J(S_{Mn1}S_{Ni2} + S_{Ni2}S_{Mn3})$ for **NiMn$_2$**, $H = -2J(S_{Fe1}S_{Ni2} + S_{Ni2}S_{Fe3})$ for **NiFe$_2$**][23] above the temperature

(23) Kahn, O. *Molecular Magnetism*; VCH Publishers: Weinheim, 1993.

of 30 K to avoid the influence of the zero-field splitting. The least-squares calculation yielded best fit parameters of $g = 2.03(1)$ and $J = +0.13(2)$ cm^{-1} for **NiMn$_2$** and $g = 2.09(1)$ and $J = +0.37(1)$ cm^{-1} for **NiFe$_2$**.

Figure 3b shows the temperature dependence of $\Delta\chi_m T$ values, which are calculated by subtraction of $\chi_m T$ for **FeFe$_2$** from $\chi_m T$ for **NiFe$_2$** and are considered to be free from the influence of the zero-field splitting of the terminal Fe(II) ions. Ferromagnetic behavior is clearly revealed, and the theoretical curve by using the above-mentioned parameters reproduce the experimental $\Delta\chi_m T$ curve.

Propagation of the ferromagnetic interaction in **NiMn$_2$** and **NiFe$_2$** can be understood by the orbital orthogonality of the spin orbitals. The central Ni(II) ion has two dσ spins on e_g orbitals in O_h formalism directing toward N-donor atoms, meanwhile terminal Fe(II) and Mn(II) ions have both dσ spins on e_g orbitals directing toward O-donor atoms and dπ spins on t_{2g} orbitals avoiding O-donor atoms, respectively. In these complexes, e_g(Ni) and e_g($M_{terminal}$) orbitals have different symmetry about 2-fold rotation around the Ni$-$N$_{amide}-M_{terminal}$ axis. The former is symmetric, whereas the latter is antisymmetric, and hence, these two e_g orbitals are orthogonal to each other. This orthogonality is advantageous to the ferromagnetic coupling between the central Ni(II) ion and the terminal Fe(II) or Mn(II) ion. On the other hand, e_g(Ni) and t_{2g}($M_{terminal}$) are symmetric with respect to rotation around the 2-fold axis and have a nonzero overlap integral that leads to a weak antiferromagnetic interaction. The weak ferromagnetic interaction in **NiMn$_2$** and **NiFe$_2$** could arise from the sum of these two opposite interactions; the through-space interaction (e_g(Ni)$-t_{2g}$($M_{terminal}$)) should be weaker than the through-bond interaction (e_g(Ni)$-e_g$($M_{terminal}$)), and the latter is slightly predominant to realize a weak ferromagnetic interaction. In the previous paper, we reported another type of linear complexes, the trinuclear $[Fe^{II}(H_2O)_2\{Fe^{III}(bpca)_2\}_2]^{4+}$ and one-dimensional *catena*-$[Fe^{II}(ClO_4)_2\{Fe^{III}(bpca)_2\}]^+$, both of which contain an alternate arrangement of high-spin Fe(II) and low-spin Fe(III) ions.[9] The observed interaction between high-spin Fe(II) and low-spin Fe(III) in these compounds was of antiferromagnetic type, and the mechanism of the interaction is explained in the same way as for the present **NiMn$_2$** and **NiFe$_2$** complexes. The lack of dσ spin on the low-spin Fe(III) sites has led to the antiferromagnetic interaction. The ferromagnetic interaction in **NiFe$_2$** (0.37 cm^{-1}) was stronger than that in **NiMn$_2$** (0.17 cm^{-1}), and the reason may be the difference between $M_{terminal}-O_{bpca}$ coordination distances as well as the difference in the number of antiferromagnetic pathways, i.e., the difference in the number of dπ electrons in Fe(II) and Mn(II) ions.

Conclusion

We succeeded in obtaining the trinuclear complexes $[M(bpca)_2\{M'(hfac)_2\}_2]$ constructed with the complex ligand $[M(bpca)_2]$. We showed the change of the electronic state of the O$-$C$-$N$-$C$-$O moiety upon formation of trinuclear complexes by X-ray crystal structure analyses and IR spectra. The magnetic behavior for **NiMn$_2$** and **NiFe$_2$** shows the ferromagnetic interaction between Ni(II) ion and M′ ion (M′ = Mn(II) and Fe(II)), which is explained in terms of the orbital orthogonality of magnetic orbitals on these metal ions.

Acknowledgment. This work was supported by Grant-in-Aid for Scientific Research on Priority Areas (No. 10149102) and by Encouragement of Young Scientists (No. 13740370) from the Ministry of Education, Science and Culture, Japan, as well as by JSPS Research Fellowships for Young Scientists (No. 6281).

Supporting Information Available: A table of selected bond angles for five compounds (Table S1) and five X-ray crystallographic files in CIF format. This material is available free of charge via the Internet at http://pubs.acs.org.

IC010731F